Scientific Research Publishing

Open Journal of Physical Chemistry, 2022, 12, 47-70
https://www.scirp.org/journal/ojpc
ISSN Online: 2162-1977
ISSN Print: 2162-1969

Combining Experimental and Quantum Chemical Study of 2-(5-Nitro-1,3-Dihydro Benzimidazol-2-Ylidene)-3-Oxo-3-(2-Oxo-2H-Chromen-3-yl) Propanenitrile as Copper Corrosion Inhibitor in Nitric Acid Solution

Mougo André Tigori[1*], Aboudramane Koné[1], Bamba Souleymane[1], Doumadé Zon[2], Drissa Sissouma[3], Paulin Marius Niamien[3]

[1]Laboratoire des Sciences et Technologies de l'Environnement, UFR Environnement, Université Jean Lorougnon Guédé, Daloa, Côte d'Ivoire
[2]UFR des Sciences Biologiques, Université Péléforo Gon Coulibaly, Korhogo, Côte d'Ivoire
[3]Laboratoire de Constitution et de Réaction de la Matière, UFR SSMT, Université Félix Houphouët-Boigny, Abidjan, Côte d'Ivoire
Email: *tigori20@yahoo.fr

How to cite this paper: Tigori, M.A., Koné, A., Souleymane, B., Zon, D., Sissouma, D. and Niamien, P.M. (2022) Combining Experimental and Quantum Chemical Study of 2-(5-Nitro-1,3-Dihydro Benzimi-dazol-2-Ylidene)-3-Oxo-3-(2-Oxo-2H-Chromen-3-yl) Propanenitrile as Copper Corrosion Inhibitor in Nitric Acid Solution. *Open Journal of Physical Chemistry*, **12**, 47-70.
https://doi.org/10.4236/ojpc.2022.124004

Received: October 15, 2022
Accepted: November 26, 2022
Published: November 29, 2022

Abstract

Due to acidic solutions aggressiveness, corrosion inhibitors use is considered to be one the most practical methods to delay metals dissolution in the said solutions. In this study benzimidazolyl derivative namely 2-cyanochalcones 2-(5-nitro-1,3-dihydrobenzimidazol-2-ylidene)-3-oxo-3-(2-oxo-2H-chromen -3-yl) propanenitrile which was synthesized was then applied as a corrosion inhibitor for copper in 1 M HNO_3 solution. The inhibition action of this molecule was evaluated by gravimetric and density functional theory (DFT) methods. It was found experimentally that this compound has a better inhibition performance and its adsorption on copper surface follows Langmuir adsorption isotherm. This adsorption evolves with temperature and inhibitor concentration, it is endothermic and occurs spontaneously with an increase in disorder. Corrosion kinetic parameters analysis supported by Adejo-Ekwenchi model revealed the existence of both physisorption and chemisorption. DFT calculations related that compound adsorption on copper surface is due to its electron donating and accepting capacity. The reactive regions specifying the electrophilic and nucleophilic attack sites were analyzed using Fukui and dual descriptor functions. Experimental results obtained were compared with the theoretical findings.

Keywords

2-Cyanochalcones2-(5-Nitro-1,3-Dihydrobenzimidazol-2-Ylidene)-3-Oxo-3-(2-Oxo-2H-Chromen-3-Yl) Propanenitrile, Copper, HNO_3 Solution, Gravimetric, Density Functional Theory

1. Introduction

Inhibitors corrosion search has become a sensitive issue [1] [2]. Although corrosion degrades certain materials and metal equipment, it is necessary to find inhibitors capable of reducing this phenomenon without harming the community and creating damage to environment. In fact, some inorganic substances including phosphates, chromates, dichromates, silicates, bromates, arsenates, tungstates, molybdates, chlorides and their derivatives were used for a long time to combat metals dissolution. Unfortunately these compounds [3] are mostly carcinogenic and pollute environment.

The current trend is to search for non-toxic organic molecules for metal inhibition corrosion, in accordance with the standards governing environmental protection [4] [5] [6] [7]. Thus this constraint has led several researchers to be interested in pharmaceutical and plant extracts molecules to prevent metals corrosion [8] [9] [10] [11]. Copper, which is a metal massively used because of its excellent mechanical and chemical properties, is not spared to corrosion [12] [13]. During its use, copper is covered with impurities or corrosion products. The removal of these corrosion products requires acidic solutions because they are often difficult to clean. These cleaning operations require some acids such as nitric acid. These acids often dissolve copper equipment, thus affecting the users on a safety and economic level.

Based on all this information, it is advisable to consider copper protection against corrosion by the use of inhibitors based on drugs or plant extracts which are generally very low toxicity and stable at high temperatures [14] [15] [16]. Some drugs such as antibacterial drugs [17], diclofenac sodium drug [18], paracetamol [8], melatonin drug [19], azithromycin [20], and vitamins [4] have been used to inhibit corrosion of metals.

For this reason, 2-(5-nitro-1,3-dihydrobenzimidazol-2-ylidene)-3-oxo-3-(2-oxo-2H-chromen-3-yl) propanenitrile was chosen for this work in order to evaluate its influence in corrosive environment to mitigate copper dissolution. This compound is derived from benzimidazolyl 2-cyanochalcones, it is a drug with the ability to treat infections caused by microscopic fungi and yeasts [21]. This molecule which has a therapeutic function could meet the standards of non-toxicity and environmental regulations based on eco-friendly and biodegradable. In addition, this molecule has in its molecular structure oxygen (O) and nitrogen (N) atoms which according to the literature [6] [9] can facilitate electronic transactions between inhibitor and copper.

It turns out that despite the high cost of experimental methods, these different electronic transactions between metal and inhibitor remain unexplained. However, density functional theory, which is a low cost computational method, is currently being used more and more to explain the inhibition mechanism [22] [23]. This theory relates that molecule inhibition performance depends on the protective layer quality which resulting from the chemical bond between metal and inhibitor molecules [24] [25].

In this work, it seems appropriate to study the inhibition power of this synthesized organic molecule which is 2-(5-nitro-1,3-dihydrobenzimidazol-2-ylidene)-3-oxo-3-(2-oxo-2H -chromen-3-yl) propanenitrile on copper corrosion in 1 M HNO_3 solution by using combined experimental and theoretical approaches.

2. Experimental

2.1. Inhibitor Synthesis Process

The inhibitor used in this work was 2-(5-nitro-1,3-dihydrobenzimidazol-2-ylidene)-3-oxo-3-(2-oxo-2H-chromen-3-yl) propanenitrile (NDCP). Its preparation consists in first reacting ortho-phenylenediamines with ethyl cyanoacetate used as reagent and solvent. The product obtained is brought to reflux in toluene with 2-oxo-2H-chromene-3-carbonyl chloride presence. After precipitation, the precipitate obtained is filtered and recrystallized in water [26]. This synthesis process is illustrated by the following reaction scheme (Scheme 1):

Physico-chemical properties: NMR 1H, 13C (DMSO-d6, δ ppm):

- 1H NMR: (300 MHz, DMSO-d6, δ ppm): 12.98 (2H, br s, NH); 8.57 (1H, s, CO-C=CH)
- 13C NMR: (75 MHz, DMSO-d6, δ ppm): 187.0 (C=O ketone); 115.8 (C≡N); 63.5 (C=C-CN)

Figure 1 indicates synthesized molecule appearance.

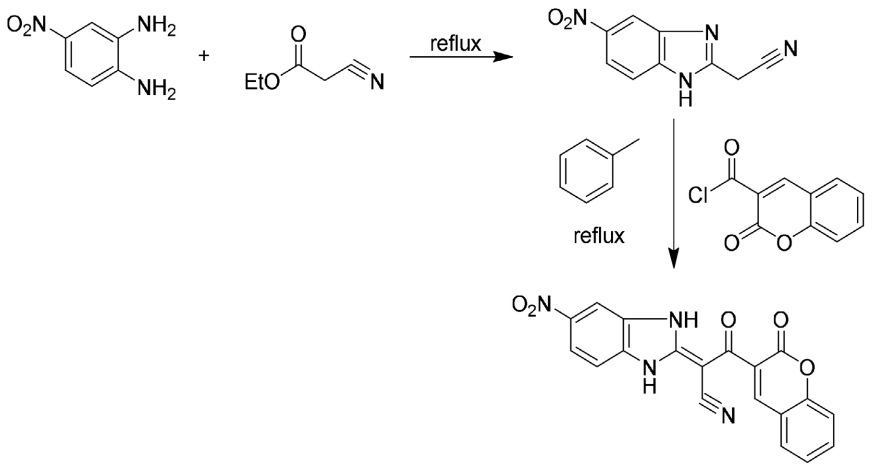

Scheme 1. Synthesis procedure of 2-(5-nitro-1,3-dihydrobenzimidazol-2-ylidene)-3-oxo-3-(2-oxo-2H-chromen-3-yl) propanenitrile (NDCP).

Figure 1. Images of a synthesized sample of NDCP.

2.2. Chemicals

The essential chemicals used for copper samples treatment are:

- ✓ HNO_3 from Merck with purity: 70% nitric. Using this commercial solution, a 1 M concentration serving as a blank for various tests was prepared.
- ✓ Acetone from Sigma Aldrich with purity: 99.5% was used to degrease copper coupons

2.3. Copper Pretreatment

Copper coupons were in form of rod measuring 10 mm in length and 2.2 mm of diameter; they were cut in commercial copper of purity 99.5%. To perform copper coupons pretreatment, these coupons were successively polished with fine quality emery papers with grain ranging from 150 to 600, cleaned in acetone, washed with double distilled water, then dried in a proofer (ASTEL) and weighed (m_1).

2.4. Gravimetric Measurements

Initially pre-treated copper coupons were completely immersed in an Erlenmeyer flask containing 50 mL of 1 M HNO_3 without and with different concentrations 2-(5-nitro-1,3-dihydrobenzimidazol-2-ylidene)-3-oxo-3-(2-oxo-2H-chromen-3-yl) propanenitrile. After one hour immersion, the coupons retrieved, washed again with double distilled water, dried in a proofer before re-weighing (m_2). The tests were repeated at temperatures ranging from 298 K to 323 K. The temperature was controlled by a thermostat water bath (Frigitherm) and an analytical balance from KERN & SOHN GmbH (precision: ±0.1 mg) was used to perform the weighing. The mass loss (Δm) was the difference of initial mass of pre-treated coupons and the mass immersed in the blank solution without or with NDCP after treatment. This mass loss is the average value from the repetition of each test. From the mass loss results, the parameters such as corrosion rate (W), surface coverage (θ) and inhibition efficiency (IE) were calculated. The expressions for the calculation of these parameters are outlined as follows:

$$W = \frac{\Delta m}{S \cdot t} = \frac{m_1 - m_2}{S \cdot t} \quad (1)$$

$$\theta = \frac{W_0 - W}{W_0} \quad (2)$$

$$IE(\%) = \frac{W_0 - W}{W_0} * 100 \quad (3)$$

Δm: mass loss (g) m_1 and m_2 are respectively, the mass (g) before and after immersion in the solution test; t: immersion time (h); S: total surface of coupon (cm^2); w_0 and w; are respectively copper corrosion rates in the absence and presence of NDCP.

2.5. Quantum Chemical Computations

To evaluate molecule adsorption properties, DFT (Density functional theory) method were used in this work. The choice of this method is based on electronic correlation consideration where the wave function is replaced by electronic density. The exchange and correlation contributions are commonly treated separately and then combined to give a complete functional. Functionals that permits to link the electron density to energy are determined to access the calculations. This method reaches similar results to other methods (ab initio, Hartree-Fock, post Hartree-Fock.) with less computation time. All calculations were performed by Gaussian 09 W [27] software using B3LYP functional with three-parameter Becke (B3) Lee-Yang-Parr [28] [29], whose analytical form is given by the following relation:

$$E_{XC}^{B3LYP} = E_{XC}^{LDA} + a_0\left(E_X^{HF} - E_X^{LDA}\right) + a_X\left(E_X^{GGA} - E_X^{LDA}\right) + a_C\left(E_C^{GGA} - E_C^{LDA}\right) \quad (4)$$

where $a_0 = 0.20$ $a_X = 0.72$ $a_C = 0.81$.

To obtain a good accuracy and precision in these theoretical computations results and geometry optimization, basis 6 - 31 G (d, p) was used. The optimized minimum energy geometrical configuration using Gauss-View 5 software and NDCP molecular are given by Figure 2.

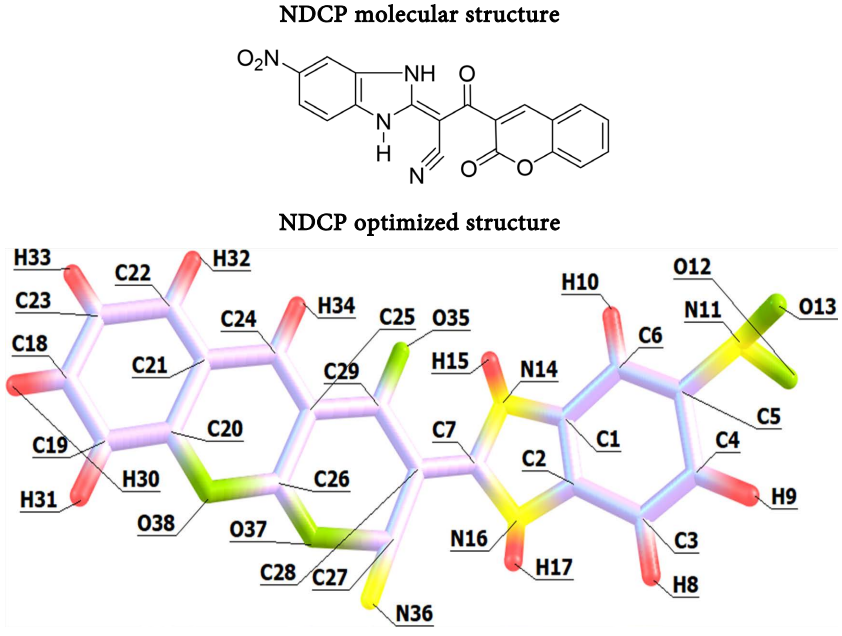

Figure 2. NDCP molecular and optimized structures.

Quantum chemical parameters involved in NDCP inhibition mechanism that were determined by this technique are: highest occupied molecular orbital energy (E_{HOMO}), lowest unoccupied molecular orbital energy (E_{LUMO}), energy gap ($\Delta E = E_{LUMO} - E_{HOMO}$), dipole moment ($\mu$), total energy ($E_T$) electron affinity ($A = -E_{LUMO}$) [30], ionization energy ($I = -E_{HOMO}$) [30]. Some parameters such electronegativity (χ), hardness (η) softness (σ) affinity and electrophylicity index (ω) are related to ionization energy (I) and electron affinity (A). They are expressed from the following relationships [31] [32]:

$$\chi = \frac{I + A}{2} \tag{5}$$

$$\eta = \frac{I - A}{2} \tag{6}$$

$$\sigma = \frac{1}{\eta} \tag{7}$$

$$\omega = \frac{(I + A)^2}{4(I - A)} \tag{8}$$

Fraction of electron transferred (ΔN) from the inhibitor to copper surface was computed according to the following relation [33]:

$$\Delta N = \frac{\chi_{cu} - \chi_{inh}}{2(\eta_{cu} + \eta_{inh})} \tag{9}$$

where $\chi_{cu} = 4.98$ eV [34] and $\eta_{cu} = 0$ [35].

NDCP local selectivity parameters such as Fukui functions and dual descriptor responsible for nucleophilic and electrophilic attacks was also determined [36] [37] [38]. The following equations were used to determine these parameters:

$$f_k^+ = \left[q_k(N+1) - q_k(N)\right] \tag{10}$$

$$f_k^- = \left[q_k(N) - q_k(N-1)\right] \tag{11}$$

$$\Delta f_k(r) = f_k^+ - f_k^- \tag{12}$$

where f_k^+ and f_k^- are respectively nucleophilic and electrophilic Fukui functions, $q_k(N+1)$, $q_k(N)$ and $q_k(N-1)$ are the electronic population of atom k in $(N+1)$, N and $(N-1)$ electrons systems.

3. Results and Discussion

3.1. Gravimetric Results Interpretation

In order to have significant information about NDCP effect in copper corrosion, gravimetric tests were carried out. The results of these tests have permitted to plot the evolution of corrosion rate (W) and the inhibition efficiency (IE) as a function of NDCP concentration and corrosive solution temperature. These plots are illustrated in **Figure 3** and **Figure 4**.

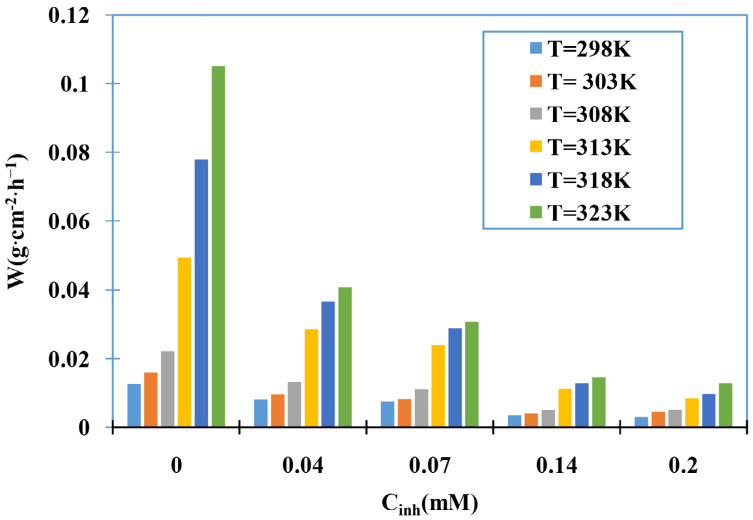

Figure 3. Corrosion rate versus NDPC concentration for various temperatures.

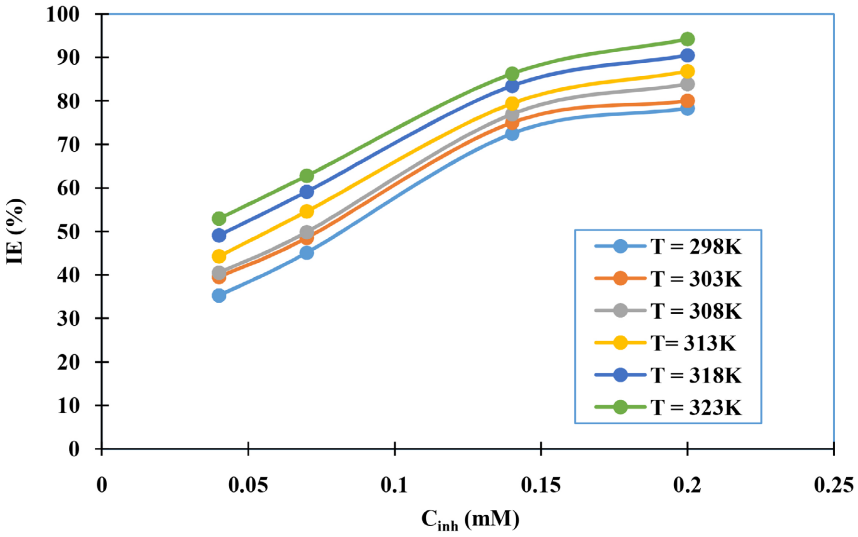

Figure 4. NDPC Inhibition efficiency (*IE*) versus concentrations for different temperatures.

It can be seen in **Figure 3** that corrosion rate increases with increasing corrosive medium temperature and NDCP absence, while this rate decreases considerably in NDCP presence. Although the increase in temperature favors copper oxidation, it is clear that for high temperatures, NDCP presence extremely reduces copper dissolution. This dissolution is characterized by Cu^{2+} ions formation in reaction medium.

Figure 4 analysis shows that inhibition efficiency increases both increasing concentration and temperature. These observations relate that when temperature evolves, Cu^{2+} ions are massively produced. So, NDCP presence in nitric solution promotes a protective layer formation with these ions. This protective whose thickness depends on NDCP concentration and which forms on copper surface, preserves it from the aggressive environment, thus reducing its dissolu-

tion. However, increasing temperature and concentration facilitates NDCP adsorption on copper surface.

Based on the above results, it was found that at low concentration and high temperatures copper dissolution is completely reduced by NDCP. Moreover, for at T = 323 K and with C_{inh} = 0.2 mM, NDCP inhibition efficiency is 92.20%. Similar results were obtained by previous studies [8] [39] [40] [41].

3.2. Adsorption Isotherm and Thermodynamic Adsorption Parameters

Gravimetric results attest that copper corrosion inhibition comes from NDCP adsorption on said metal surface. It is then necessary to determine the isotherm model and thermodynamic adsorption parameters which permit to judge NDCP absorptive behavior.

To find the isotherm model suitable for NDCP behavior, several attempts have been made at some ordinary isotherms which are El-Awady, Freundlich, Temkin, Langmuir and Frumkin. The fits obtained with different graphs indicate that experimental data from gravimetric measurements are in better agreement with Langmuir isotherm. Indeed, regression coefficient (R^2) of straight lines obtained during the study of this model are closer to unit. Langmuir adsorption isotherm is provided by following corresponding equation [42]:

$$\frac{C_{inh}}{\theta} = \frac{1}{K_{ads}} + C_{inh} \tag{13}$$

C_{inh}: inhibitor concentration; K_{ads}: adsorption equilibrium constant; θ: surface coverage rate.

This model representation is given by the plot of C_{inh}/θ versus C_{inh} (**Figure 5**).

Moreover, the standard free energy of adsorption which is a thermodynamic parameter can be calculated according to the following relation [43]:

$$\Delta G_{ads}^{0} = -RT \ln\left(55.5 K_{ads}\right) \tag{14}$$

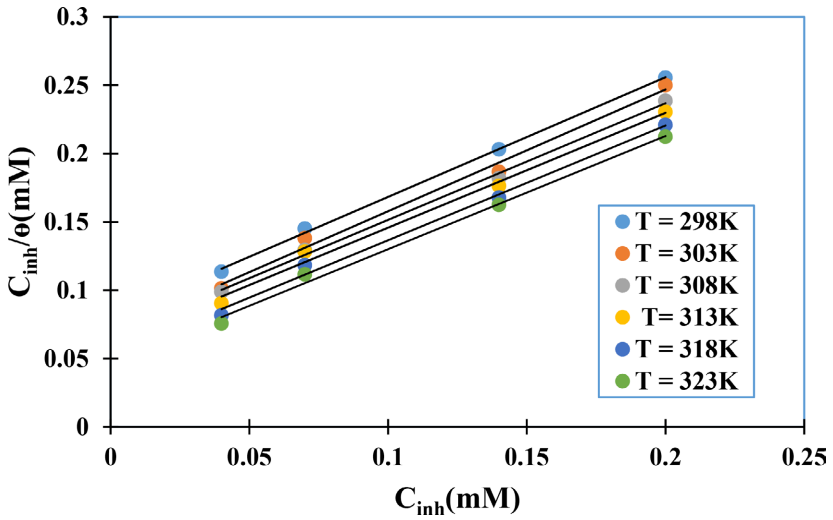

Figure 5. Langmuir adsorption isotherm of NDCP.

where R is gas constant, T is absolute temperature, K_{ads} adsorption equilibrium constant and 55.5 is water concentration (mol/L) in solution.

Standard adsorption enthalpy (ΔH_{ads}^{0}) and entropy (ΔS_{ads}^{0}) are determined by applying the following equation [44]:

$$\Delta G_{ads}^{0} = \Delta H_{ads}^{0} - T\Delta S_{ads}^{0} \quad (15)$$

Figure 6 illustrates the plot of ΔG_{ads}^{0} versus temperature. ΔH_{ads}^{0} and ΔS_{ads}^{0} values were determined respectively from the intercept and the slope of the straight line obtained. All the quantities related to Langmuir isotherm and thermodynamic adsorption parameters are listed in Table 1.

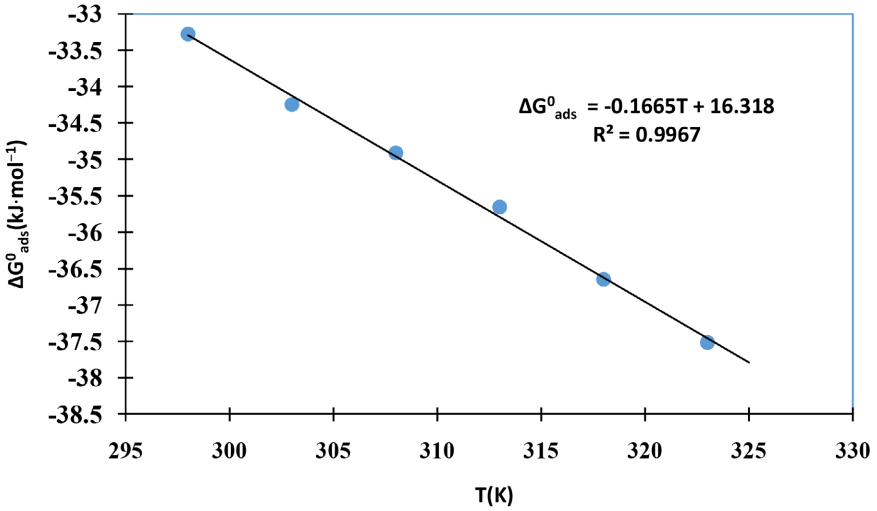

Figure 6. Evolution of ΔG_{ads}^{0} as a function of temperature.

Table 1. NDCP adsorption parameters obtained by gravimetric estimations.

T (K)	Equations	R^2	$K_{ads}.10^3$ (M^{-1})	ΔG_{ads}^{0} (kJ·mol^{-1})	ΔG_{ads}^{0} (kJ·mol^{-1})	ΔS_{ads}^{0} (J·mol^{-1}·K^{-1})
298	$\frac{C_{inh}}{\theta} = 0.876C_{inh} + 0.0808$	0.998	12.36	−33.279		
303	$\frac{C_{inh}}{\theta} = 0.8915C_{inh} + 0.0687$	0.991	14.556	−34.249		
308	$\frac{C_{inh}}{\theta} = 0.8537C_{inh} + 0.0661$	0.997	15.128	−34.913		
					16.318	166.5
313	$\frac{C_{inh}}{\theta} = 0.8404C_{inh} + 0.0618$	0.99	16.181	−35.655		
318	$\frac{C_{inh}}{\theta} = 0.8403C_{inh} + 0.0526$	0.993	19.011	−36.650		
323	$\frac{C_{inh}}{\theta} = 0.8286C_{inh} + 0.0472$	0.994	21.186	−37.517		

A review of Table 1 relates that the slopes of straight lines obtained are approximately equal to unity. In this case, NDCP adsorbs on copper according to Langmuir isotherm. This isotherm mentions that there is a fixed number of sites on copper surface and that each of these sites can adsorb only one particle, it is thus that a monolayer of NDCP is adsorbed on metal surface. Moreover, the interactions between adsorbed NDCP particles and metal surface are negligible and adsorption energy is constant.

As can be seen in Table 1, the negative ΔG_{ads}^{0} values suggest that NDCP adsorption onto copper is spontaneous and the layer from this adsorption is stable [45]. The results relating to ΔG_{ads}^{0} attest that the values of this quantity are between −20 kJ/mol and −40 kJ/mol, thus translating the existence of two adsorption modes: chemisorption and physisorption [45]. These adsorption modes indicate that covalent bonds are therefore established between the molecule and the metal surface as well as electrostatic interactions between the inhibitor and copper surface. As for the values of standard adsorption enthalpy (ΔH_{ads}^{0}) and entropy (ΔS_{ads}^{0}), they are positive, this translates respectively the endothermic character of NDCP adsorption and increasing disorder during NDCP molecules adsorption on copper surface [17]. This disorder is caused by water molecules desorption.

3.3. Corrosion Kinetic Analysis

Gravimetric tests proved that NDCP inhibition efficiency depends on temperature variations. These results confirm that the temperature is an element allowing to control copper dissolution process in the presence and absence of NDCP. Thus kinetic parameters of this process were determined from Arrhenius relationship and the transition state described as follows [46]:

$$\log W = \log A - \frac{E_a}{2.3RT} \tag{16}$$

$$\log\left(\frac{W}{T}\right) = \log\left(\frac{R}{\aleph h}\right) + \frac{\Delta S_a^*}{2.3R} - \frac{\Delta H_a^*}{2.3RT} \tag{17}$$

W: corrosion rate, E_a: activation energy of metal dissolution reaction, R: universal gas constant, T: temperature, A: Arrhenius preexponential constant.

ΔS_a^*: activation entropy, ΔH_a^*: activation enthalpy, R universal gas constant, $\aleph$: Avogadro number, h: Planck's constant.

Figure 7 shows the plot of $\log W$ versus $\frac{1}{T}$. The slopes of the straight lines $\left(-\frac{E_a}{2.3R}\right)$ obtained permit to determine activation energy (E_a) in absence and presence of NDCP. ΔH_a^* and ΔS_a^* are determined from the plot of $\log\left(\frac{W}{T}\right)$ versus $\frac{1}{T}$, where the slopes $\left(-\frac{\Delta H_a^*}{2.3R}\right)$ and intercepts $\left(\log\left(\frac{R}{\aleph h}\right) + \frac{\Delta S_a^*}{2.3R}\right)$ of the straight lines (Figure 8) lead to respective values of ΔH_a^* and ΔS_a^*. The values of the different activation quantities are recorded in Table 2.

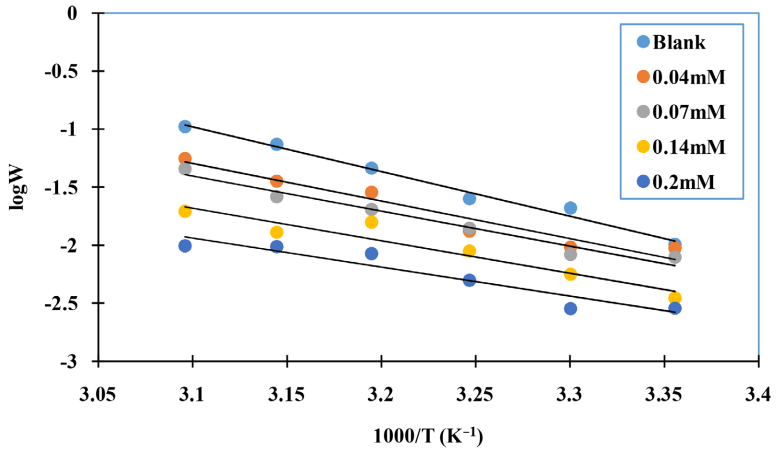

Figure 7. $\log W$ versus $\frac{1}{T}$.

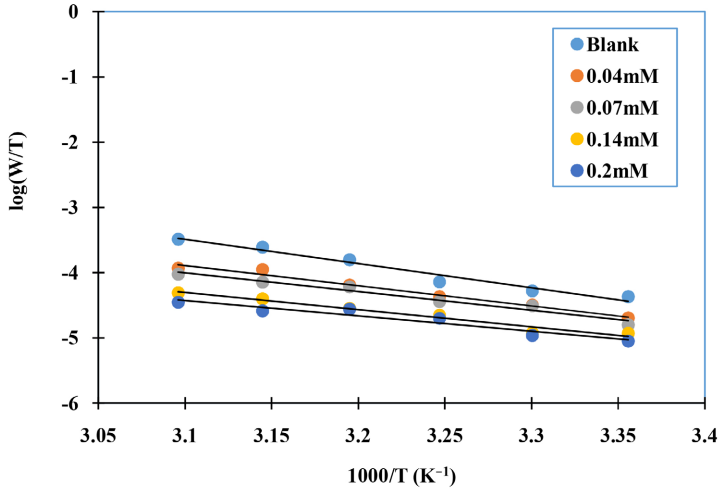

Figure 8. $\log\left(\frac{W}{T}\right)$ versus $\frac{1}{T}$.

Table 2. Activation parameters of copper dissolution in 1 M HNO_3.

C_{inh} (mM)	E_a (kJ·mol^{-1})	ΔH_a^* (kJ·mol^{-1})	$E_a - \Delta H_a^*$ (kJ·mol^{-1})	ΔS_a^* (J·mol^{-1}·K^{-1})
Blank	73.62	70.99	2.63	−44.23
0.04	61.95	59.38	2.57	−87.84
0.07	57.46	54.94	2.59	−103.75
0.14	52.89	50.20	2.69	−124.23
0.2	47.83	45.05	2.78	−109.04

Inspection of the results obtained show that the activation energy (E_a) decreases as inhibitor concentration increases. It was observed that (E_a) value in blank solution is higher than the values of E_a in NDCP presence. The decrease of

E_a in inhibited solutions attests that copper dissolution is strongly attenuated in NDCP presence [47]. Indeed in the corrosive solution copper dissolves rapidly by losing electrons, which electrons are replaced by those of the inhibitor from heteroatoms (N, O) and π bonds. These findings translate that NDCP is absorbed chemically on copper surface. Furthermore activation energy values of dissolution process in absence and NDCP presence are greater than 20 kJ·mol^{-1}, which means that the whole process is controlled by the surface reaction [47]. In this case, it appears that chemical and physical adsorption are present during NDCP inhibition process and this is done mainly by chemical adsorption. Activation enthalpy values are positive mentioning the endothermic character of copper dissolution process of in the absence and presence of NDCP [48]. These values decrease in NDCP presence, it reveals that copper dissolution becomes slow in studied molecule presence. It is also found that the difference: $E_a - \Delta H_a^*$ is practically constant, translating that E_a and ΔH_a^* vary in the same way. Consequently, this result obeys the thermodynamic relation between these two quantities: $E_a - \Delta H_a^* = RT$ [49]. Negative values of ΔS_a^* which decrease in NDCP presence reveal that Cu-inhibitor complex formation considerably reduces the disorder created by water molecules desorption [48].

3.4. Adsorption Type Analysis

Adsorption and activation parameters have meant that both types of adsorption exist in NDCP inhibition. To have complete information to distinguish physisorption and chemisorption, Adejo-Ekwenchi isotherm has been used [50]. The relationship that characterizes this isotherm is reported below.

$$\log\left(\frac{1}{1-\theta}\right) = \log K_{AE} + b\log C_{inh} \tag{18}$$

The representation associated with this model is exemplified in **Figure 9**. The parameters corresponding to this model are listed in **Table 3**.

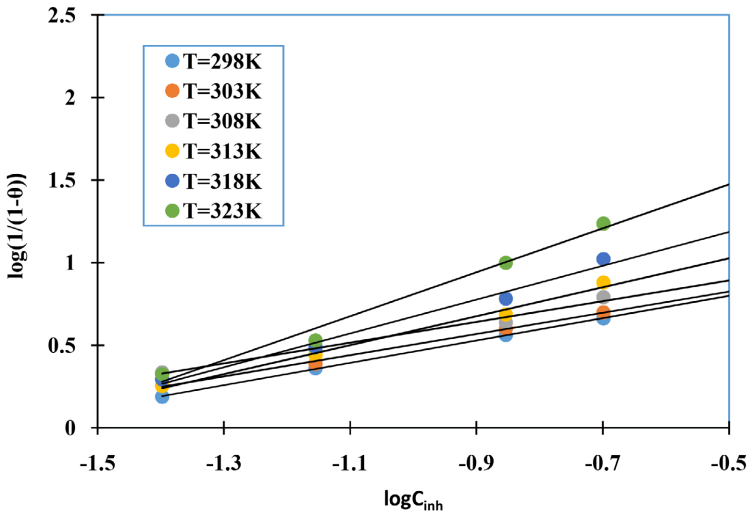

Figure 9. Adejo-Ekwenchi adsorption model plots for NDCP for various temperatures.

Table 3. Adejo-Ekwenchi model parameters.

T(K)	Equation	R^2	b	K_{AE}
298	$\log\left(\frac{1}{1-\theta}\right) = 0.6766\log C_{inh} + 1.1377$	0.9997	0.6766	13.7309
303	$\log\left(\frac{1}{1-\theta}\right) = 0.6415\log C_{inh} + 1.1453$	0.9968	0.6415	13.9733
308	$\log\left(\frac{1}{1-\theta}\right) = 0.6275\log C_{inh} + 1.2054$	0.9858	0.6275	16.0472
313	$\log\left(\frac{1}{1-\theta}\right) = 0.8753\log C_{inh} + 1.4638$	0.9912	0.8753	29.0938
318	$\log\left(\frac{1}{1-\theta}\right) = 1.0238\log C_{inh} + 1.6976$	0.9843	1.0238	49.8425
323	$\log\left(\frac{1}{1-\theta}\right) = 1.3305\log C_{inh} + 2.1386$	0.9839	1.3305	137.5941

According to the results from Adejo-Ekwenchi model (**Table 3**), it appears that parameter b values decreases from 298 K to 308 K. This decrease relates that NDCP adsorbs on copper surface by electrostatic bonds in range of 298 K to 308 K [50]. Inhibition efficiencies values obtained by means of gravimetric tests in this range of temperatures are low. These results attest that the electrostatic interactions that occur therefore do not properly promote good corrosion inhibition of copper, because these electrostatic bonds are weak and are sensitive to temperature increase. In contrast, for temperatures range from 308 K to 323 K, parameter b increases, indicating that NDCP adsorbs onto metal surface through chemical bonds [50]. These bonds are formed by electron sharing between NDCP molecules and unsaturated copper d-orbitals, thus forming covalent bonds that are strong bonds. These bonds allow to maintain a good inhibition efficiency when the temperature increases, which justifies the high IE% values obtained at high temperature.

3.5. Quantum Chemical Interpretation

3.5.1. Global Reactivity and HOMO-LUMO Orbitals

Gravimetric estimations revealed that NDCP has a good inhibition performance. This performance is due to its absorptive properties. In order to deepen the inhibition mechanism characteristics, quantum chemical calculations were performed. Thus, the global parameters resulting from these calculations were requested to explain experimental results obtained and to better understand NDCP inhibition action. These parameters were determined with DFT at B3LYP/6-31G (d, p) basis set and are recorded in **Table 4**.

An organic compound reactivity depends on its ability to donate or receive electrons [51]. The parameters indicative of electron donation and acceptance are respectively HOMO and LUMO orbitals energies [52]. Indeed, according to

Table 4. NDCP global reactivity parameters calculated using B3LYP/6-31G(d, p).

Global parameters	Value	Global parameters	Value
E_{HOMO} (eV)	−6.083	χ (eV)	4.402
E_{LUMO} (eV)	−2.720	η (eV)	1.682
ΔE (eV)	3.363	σ (eV)$^{-1}$	0.147
μ (*D*)	6.303	ΔN	0.172
I (eV)	6.083	ω	5.761
A (eV)	2.720	E_T (Ha)	−1325.08

the values obtained in literature [53] [54] it was found that NDCP E_{HOMO} value is high, which results in NDCP having a greater ability to donate electrons to copper which has low energy empty molecular orbitals. In contrast, a lower E_{LUMO} value as displayed by the one obtained with NDCP means that this molecule is likely to accept electrons from copper appropriate occupied orbitals. These donation and acceptance properties that NDCP possesses justify its strong adsorption to copper surface. An organic compound reactivity evolution is also controlled by energy gap (ΔE). In effect when ΔE decreases, molecule reactivity increases and when ΔE increases molecule reactivity decreases [55]. ΔE value obtained in this study reveals that the electronic exchanges molecule-copper are very favorable, which contributes to establish chemical bonds with copper. These bonds reinforce its adsorption capacity on the metal surface thus justifying the high efficiencies obtained experimentally. **Figure 10** illustrates the molecular energy gap (molecular energy gap) which permits to judge the donation and electron acceptance capacities of NDCP.

Although some authors argue that a lower dipole moment (μ) facilitates inhibitor adsorption to metal surface [56], others report that a high dipole moment, ensures a good reactivity of the molecule which can increase the corrosion inhibition efficiency [17] [57]. In our study, the value of the dipole moment for NDCP (6.303 D) comparing to other values reported in previous works is high [58] [59], which justifies the better inhibition performance of the compound in tested solution.

Molecule electron donation and acceptance properties can also be discussed with ionization potential (I) and electron affinity (A) [60]. The low value of I and high value of A displayed in **Table 4** confirms these properties for NDCP.

The electronegativity (χ) represents the electron attraction capacity of a molecule [61]. Electronegativity value obtained is lower than that of copper, this indicates NDCP electrons are strongly attracted to copper. This electron transfer is corroborated by the positive value of fraction of transferred electrons (ΔN) and low hardness (η) [62]. Therefore, the electron loss that copper undergoes in 1 M HNO_3 is systematically reduced by an electron donation from NDCP. This electron donation contributes to covalent bonds formation with copper. The high value of global softness (σ) relates that NDCP is a soft molecule therefore, it

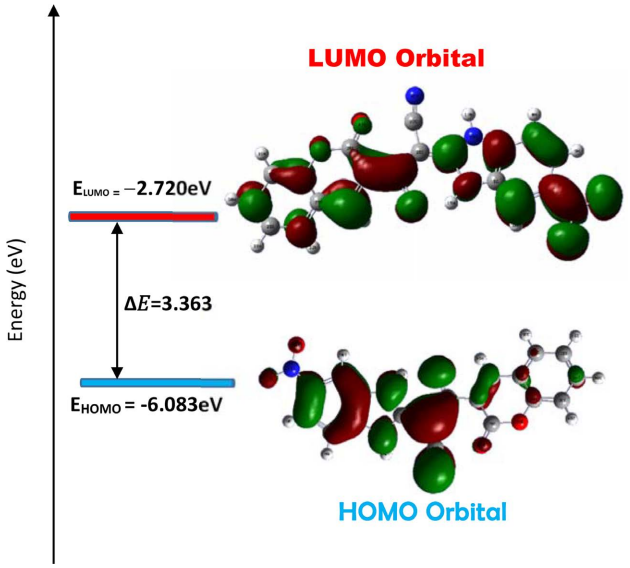

Figure 10. Energy diagram of HOMO-LUMO orbitals for NDCP.

possesses a high chemical reactivity [63]. Which high reactivity would favor its strong adsorption on copper surface hence a good inhibition efficiency.

Electrophilicity index (ω) is a parameter which permits to estimate a compound capacity to accept or to give electrons [64]. In our work high value of ω attests that NDCP is a good electrophile and has a good ability to accept electrons from copper. Global reactivity parameters certified that electron transfer from NDCP to copper and vice versa are very favorable. Negative value total energy claims this assertion [65]. Analysis global reactivity descriptors are consistent with gravimetric estimations.

3.5.2. Local Reactivity

Global reactivity study indicated that NDCP adsorption on copper surface as estimated by gravimetric tests is related to its propensity to donate and accept electrons from appropriate occupied copper orbitals. Then, it is necessary to study local molecule reactivity. This reactivity consists in locating within molecule the atoms which are responsible for nucleophilic and electrophilic attacks [66]. Indeed NDCP molecular configuration indicates that this molecule has 38 atoms among which are 9 heteroatoms (N, O). The presence of these heteroatoms and aromatic rings can influence the behavior of certain atoms in the molecule. Therefore the centers of attack which permit to clarify the electronic properties will be elucidated by Fukui functions and dual descriptor. The values of these different parameters are listed in **Table 5**.

According to the local reactivity indices values reported in **Table 5**, C(26) and N(36) atoms are centers for electrophilic attacks associated with HOMO region and nucleophilic attacks associated with LUMO region, respectively. These centers are confirmed by f_k^- high value and the lowest value of $\Delta f_k(r)$ possessed by C(26) and the highest values f_k^+ and $\Delta f_k(r)$ that N(36) has. The most favourable reactivity sites for adsorption are indicated by **Figure 11**.

Table 5. Mulliken atomic charges, Fukui function and dual descriptor.

Atoms	$q_k(N+1)$	$q_k(N)$	$q_k(N-1)$	f_k^+	f_k^-	$\Delta f_k(r)$
1 C	0.000159	0.201174	0.002854	−0.201015	0.19832	−0.399335
2 C	0.000177	0.213238	−0.01079	−0.213061	0.224028	−0.437089
3 C	0.000072	−0.103641	0.002811	0.103713	−0.106452	0.210165
4 C	−0.00012	−0.059883	0.005026	0.059763	−0.064909	0.124672
5 C	0.000076	0.24498	0.025816	−0.244904	0.219164	−0.464068
6 C	−0.000144	−0.098763	−0.002766	0.098619	−0.095997	0.194616
7 C	−0.003025	0.438514	0.037742	−0.441539	0.400772	−0.842311
8 H	−0.000003	0.125271	0.001594	−0.125274	0.123677	−0.248951
9 H	0.000004	0.136708	0.002659	−0.136704	0.134049	−0.270753
10 H	0.000011	0.130812	0.002287	−0.130801	0.128525	−0.259326
11 N	−0.000007	0.122976	0.214432	−0.122983	−0.091456	−0.031527
12 O	−0.000051	−0.283161	0.109898	0.28311	−0.393059	0.676169
13 O	0.000062	−0.277938	0.348559	0.278	−0.626497	0.904497
14 N	−0.002343	−0.553817	0.002081	0.551474	−0.555898	1.107372
15 H	−0.000148	0.304884	−0.000082	−0.305032	0.304966	−0.609998
16 N	0.000304	−0.57007	−0.006139	0.570374	−0.563931	1.134305
17 H	0.001287	0.292721	−0.000124	−0.291434	0.292845	−0.584279
18 C	−0.003449	−0.075768	0.044967	0.072319	−0.120735	0.193054
19 C	0.011725	−0.149869	−0.012773	0.161594	−0.137096	0.29869
20 C	0.003174	0.329086	0.015824	−0.325912	0.313262	−0.639174
21 C	0.008584	0.089935	−0.02827	−0.081351	0.118205	−0.199556
22 C	−0.00875	−0.158369	0.065135	0.149619	−0.223504	0.373123
23 C	0.012632	−0.089032	−0.024583	0.101664	−0.064449	0.166113
24 C	−0.007039	−0.089971	0.145497	0.082932	−0.235468	0.3184
25 C	0.008277	−0.030399	−0.00601	0.038676	−0.024389	0.063065
26 C	0.03758	0.571332	0.017502	−0.533752	**0.55383**	**−1.087582**
27 C	0.12133	0.273712	0.003994	−0.152382	0.269718	−0.4221
28 C	0.00127	−0.050351	−0.023246	0.051621	−0.027105	0.078726
29 C	0.002477	0.407172	0.042773	−0.404695	0.364399	−0.769094
30 H	0.000166	0.110814	−0.002221	−0.110648	0.113035	−0.223683
31 H	−0.000446	0.120047	0.000392	−0.120493	0.119655	−0.240148
32 H	0.000336	0.11104	−0.002949	−0.110704	0.113989	−0.224693
33 H	−0.000523	0.104827	0.000819	−0.10535	0.104008	−0.209358

Continued

34 H	0.000454	0.143843	−0.006505	−0.143389	0.150348	−0.293737
35 O	0.013162	−0.534604	0.033759	0.547766	−0.568363	1.116129
36 N	0.531004	−0.422971	−0.011664	**0.953975**	−0.411307	**1.365282**
37 O	0.239851	−0.385651	0.006784	0.625502	−0.392435	1.017937
38 O	0.03187	−0.538825	0.00492	0.570695	−0.543745	1.11444

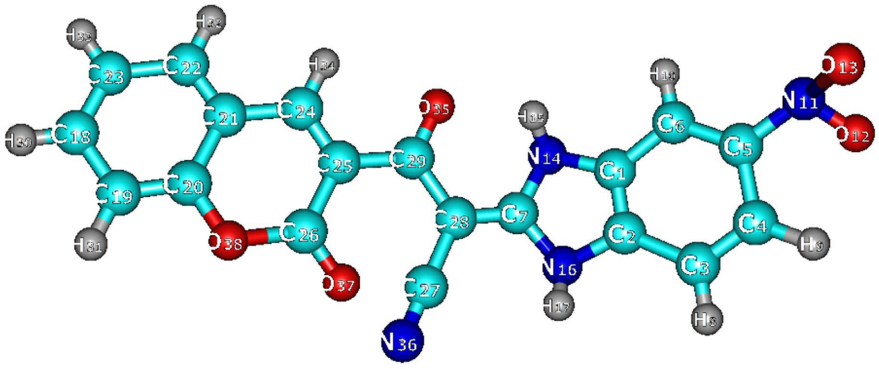

Figure 11. Optimized geometry for NDCP obtained by DFT at B3LYP/6-31G(d, p).

In fact carbon C(26) surrounded by two heteroatoms O(37) and O(38) having solitary electron pairs will be filled with electrons. Thus this electron rich site is suitable to bind to metal surface by giving electrons to Cu^{2+} ions ($[Ar]3d^9$). Whereas nitrogen N(36) which is only linked to C(27) will be depleted in electrons because of its electron pair delocalization. This site will therefore receive electrons from copper. Finally, the identified sites are responsible for chemical bonds formation.

3.5.3. Mechanism of Inhibition

Global reactivity study explained the experimental results, while NDCP reactivity sites were located through local parameters. Therefore, it is significant to clarify NDCP mechanism inhibition for copper corrosion in 1 M HNO_3. In fact, copper oxidizes in 1 M HNO_3 to Cu^{2+} while NDCP inhibitor molecules can easily be protonated in the said solution according to the equation below:

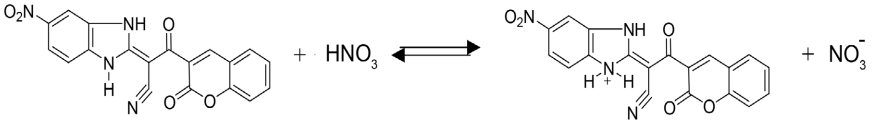

When negatively charged NO_3^- ions attach to copper surface, electrostatic interactions are created between these ions and inhibitor protonated form. Furthermore, when NDCP neutral and protonated forms adsorb onto copper surface, coordination bonds are formed. These bonds arise from donor-acceptor interactions between π-electrons of aromatic rings, N(36) and C(26) atoms of

inhibitor and copper vacant d-orbitals. This chemical adsorption process creates a protective film that will slow down copper oxidation. This protective film becomes thicker when temperature increases. Indeed, the increase of the temperature facilitates copper dissolution, thus a great Cu^{2+} ions number is created, metal electrons and those of NDCP become very mobile. This high mobility reinforces donor-acceptor interactions which increases protective film formation on copper surface, which explains the increase of inhibition efficiency at high temperature.

4. Conclusions

The following highlights were deduced from combining theoretical and experimental results obtained in this work:

- Gravimetric estimations mentioned that NDCP has good inhibition potentiality for copper corrosion in 1 M HNO_3.
- NDCP corrosion inhibition ability generally results from a protective film formation on copper surface whose thickness increases with increasing temperature and inhibitor concentration.
- NDCP adsorption on copper surface obeys Langmuir model isotherm and adsorption parameters indicate that this process is spontaneous and endothermic.
- ΔG_{ads}^{0} negative values, the activation parameters and Adejo-Ekwenchi model confirmed that NDCP adsorption on copper surface occurred chemically and physically.
- The study of the corrosion kinetic parameters permitted to verify thermodynamic relation which is: $E_a - \Delta H_a^*$
- Through DFT-based quantum chemical calculations at B3LYP/6-31-G(d, p) basis set, a correlation between the parameters related to electronic and molecular structures of NDCP and its ability to delay copper corrosion process was established
- Theoretical calculations provided a better understanding of NDCP inhibition action mechanism and are in full agreement with experimental results.
- Future work will focus on QSPR modeling (at 25˚C), which consists in establishing a mathematical relationship between quantum chemical parameters and inhibition efficiency and also perform surface studies before and after copper immersion in study solution.

Conflicts of Interest

The authors declare no conflicts of interest regarding the publication of this paper.

References

[1] Zhan, C., Ahmed, A.F., Tianqi, C., Anees, A.K., Chaoyang, F. and Noor, A.F. (2021) Green Synthesis of Corrosion Inhibitor with Biomass Platform Molecule: Gravime-

trical, Electrochemical, Morphological, and Theoretical Investigations. *Journal of Molecular Liquids*, **332**, Article ID: 115852.
https://doi.org/10.1016/j.molliq.2021.115852

[2] Hou, B.S., Xu, N., Zhang, Q.H., Xuan, C.J., Liu, H.F. and Zhang, G.A. (2019) Effect of Benzyl Substitution at Different Sites on the Inhibition Performance of Pyrimidine Derivatives for Mild Steel in Highly Acidic Solution. *Journal of the Taiwan Institute of Chemical Engineers*, **95**, 541-554.
https://doi.org/10.1016/j.jtice.2018.09.010

[3] Qiang, Y., Zhang, S. and Wang, L. (2019) Understanding the Adsorption and Anticorrosive Mechanism of DNA Inhibitor for Copper in Sulfuric Acid. *Applied Surface Science*, **492**, 228-238. https://doi.org/10.1016/j.apsusc.2019.06.190

[4] Tianqi, C., Hui, G., Zhan, C., Mengjin, C. and Chaoyang, F. (2021) Eco-Friendly Approach to Corrosion Inhibition of AA5083 Aluminum Alloy in HCl Solution by the Expired Vitamin B1 Drugs. *Journal of Molecular Structure*, **15**, Article ID: 130881. https://doi.org/10.1016/j.molstruc.2021.130881

[5] Elabbasy, H.M. and Gadow, H.S. (2021) Study the Effect of Expired Tenoxicam on the Inhibition of Carbon Steel Corrosion in a Solution of Hydrochloric Acid. *Journal of Molecular Liquids*, **1**, Article ID: 114918.
https://doi.org/10.1016/j.molliq.2020.114918

[6] Boughoues, Y., Benamira, M., Messaadia, L. and Ribouh, N. (2020) Adsorption and Corrosion Inhibition Performance of Some Environmental Friendly Organic Inhibitors for Mild Steel in HCl Solution via Experimental and Theoretical Study. *Colloids and Surfaces A*: *Physicochemical and Engineering*, **593**, Article ID: 124610.
https://doi.org/10.1016/j.colsurfa.2020.124610

[7] Deyab, M.A. (2015) Egyptian Licorice Extract as a Green Corrosion Inhibitor for Copper in Hydrochloric Acid Solution. *Journal of Industrial and Engineering Chemistry*, **22**, 384-389. https://doi.org/10.1016/j.jiec.2014.07.036

[8] Žaklina, Z., TasićMarija, B., Mihajlović, P., Radovanović, M.B., Simonović, A.T. and Antonijević, M.M. (2021) Experimental and Theoretical Studies of Paracetamol as a Copper Corrosion Inhibitor. *Journal of Molecular Liquids*, **327**, Article ID: 114817.
https://doi.org/10.1016/j.molliq.2020.114817

[9] Gao, L., Peng, S., Huang, X. and Gong, Z. (2020) A Combined Experimental and Theoretical Study of Papain as a Biological Eco-Friendly Inhibitor for Copper Corrosion in H_2SO_4 Medium. *Applied Surface Science*, **511**, Article ID: 145446.
https://doi.org/10.1016/j.apsusc.2020.145446

[10] Vandanan, S., Kumari, R. and Yadav, M. (2022) Novel Carbon Dots as Efficient Green Corrosion Inhibitor for Mild Steel in HCl Solution: Electrochemical, Gravimetric and XPS Studies. *Journal of Physics and Chemistry of Solids*, **160**, Article ID: 110341. https://doi.org/10.1016/j.jpcs.2021.110341

[11] Gökhan, G. (2011) Drugs: A Review of Promising Novel Corrosion Inhibitors. *Corrosion Science*, **53**, 3873-3898. https://doi.org/10.1016/j.corsci.2011.08.006

[12] Zhang, J., Zhang, L. and Tao, G. (2018) A Novel and High Efficiency Inhibitor of 5-(4-methoxyphenyl)-3h1,2-dithiole-3-thione for Copper Corrosion Inhibition in Sulfuric Acid at Different Temperatures. *Journal of Molecular Liquids*, **272**, 369-379.
https://doi.org/10.1016/j.molliq.2018.09.095

[13] Echihi, S., Benzbiria, N., Belghiti, M.E., *et al.* (2021) Corrosion Inhibition of Copper by Pyrazole Pyrimidine Derivative in Synthetic Seawater: Experimental and Theoretical Studies. *Materials Today Proceeding*, **37**, 3958-3966.
https://doi.org/10.1016/j.matpr.2020.09.264

[14] Zhou, L., Zhang, S., Tan, B., Feng, L., Xiang, B., Chen, F., Li, W., Xiong, B. and Song, T. (2020) Phenothiazine Drugs as Novel and Eco-Friendly Corrosion Inhibitors for Copper in Sulfuric Acid Solution. *Journal of the Taiwan Institute of Chemical Engineers*, **113**, 253-263. https://doi.org/10.1016/j.jtice.2020.08.018

[15] El-Haddad, M.N. (2013) Chitosan as a Green Inhibitor for Copper Corrosion in Acidic Medium. *International Journal of Biological Macromolecules*, **55**, 142-149. https://doi.org/10.1016/j.ijbiomac.2012.12.044

[16] Guo, L., *et al.* (2020) Eco-Friendly Food Spice 2-Furfurylthio-3-methylpyrazine as an Excellent Inhibitor for Copper Corrosion in Sulfuric Acid Medium. *Journal of Molecular Liquids*, **317**, Article ID: 113915. https://doi.org/10.1016/j.molliq.2020.113915

[17] Abdallah, M., Al Bahira, A., Altass, H.M., Fawzy, A., El Guesmi, N., Al-Gorair, A.S., Warad, F.B. and Zarrouk, A. (2021) Anticorrosion and Adsorption Performance of Expired Antibacterial Drugs on Sabic Iron Corrosion in HCl Solution: Chemical, Electrochemical and Theoretical Approach. *Journal of Molecular Liquids*, **330**, Article ID: 115702. https://doi.org/10.1016/j.molliq.2021.115702

[18] Almashhadani, H.A., Alshujery, M.K., Khalil, M., Kadhemd, M.M. and Khadom, A.A. (2021) Corrosion Inhibition Behavior of Expired Diclofenac Sodium Drug for Al 6061 Alloy in Aqueous Media: Electrochemical, Morphological, and Theoretical Investigations. *Journal of Molecular Liquids*, **343**, Article ID: 117656. https://doi.org/10.1016/j.molliq.2021.117656

[19] Jabir, H., Al-Fahemi, Abdallah, M., Elshafie, M., Gad, A.M. and Jahdaly, B.A.A. (2016) Experimental and Theoretical Approach Studies for Melatonin Drug as Safely Corrosion Inhibitors for Carbon Steel Using DFT. *Journal of Molecular Liquids*, **222**, 1157-1163. https://doi.org/10.1016/j.molliq.2016.07.085

[20] Žaklina, Z.T., Marija, B. Petrović, M., Milan, B.R. and Milan, M. (2018) Antonijević Electrochemical Investigations of Copper Corrosion Inhibition by Azithromycin in 0.9% NaCl. *Journal of Molecular Liquids*, **265**, 687-692. https://doi.org/10.1016/j.molliq.2018.03.116

[21] Djohan, V., Angora, K.E., Vanga-Bosson, A.H., Konaté, A., Kassi, F.K., Yavo, W. and Kiki Barro, P.C. (2011) *In Vitro* Susceptibility of Vaginal *Candida albicans* to Antifungal Drugs in Abidjan (Ivory Coast). *Journal de Mycologie Médicale*, **22**, 129-133. https://doi.org/10.1016/j.mycmed.2011.11.005

[22] Ryu, H.Y., *et al.* (2022) Theoretical Validation of Inhibition Mechanisms of Benzotriazole with Copper and Cobalt for CMP and Post-CMP Cleaning Applications. *Microelectronic Engineering*, **262**, Article ID: 111833. https://doi.org/10.1016/j.mee.2022.111833

[23] Xu, Y., Zhang, S., Li, W., Guo, L., Xu, S., Feng, L. and Madkour, L.H. (2018) Experimental and Theoretical Investigations of Some Pyrazolo-Pyrimidine Derivatives as Corrosion Inhibitors on Copper in Sulfuric Acid Solution. *Applied Surface Science*, **459**, 612-620. https://doi.org/10.1016/j.apsusc.2018.08.037

[24] Ma, T.D., *et al.* (2021) Multidimensional Insights into the Corrosion Inhibition of Potassium Oleate on Cu in Alkaline Medium: A Combined Experimental and Theoretical Investigation. *Materials Science and Engineering*, **272**, Article ID: 115330. https://doi.org/10.1016/j.mseb.2021.115330

[25] Hu, L.J., *et al.* (2020) The Synergistic Inhibitory Effect and Density Functional Theory Study of 2,2'-[[(Methyl-1H-benzotriazol-1-yl)methyl]imino]bisethanol and Potassium Oleate on Copper in H_2O_2 Based Alkaline Slurries. *Colloids and Surfaces A*: *Physicochemical and Engineering Aspects*, **603**, Article ID: 125275.

https://doi.org/10.1016/j.colsurfa.2020.125275

[26] Goli-Garmroodi, F., *et al.* (2015) Simple and Efficient Syntheses of Novel Benzo[4,5]imidazo[1,2-*a*]pyridine Derivatives. *Tetrahedron Letters*, **56**, 743-746. https://doi.org/10.1016/j.tetlet.2014.12.099

[27] Frisch, M.J., Trucks, G.W., Schlegel, H.B., *et al.* (2009) Gaussian 09. Gaussian, Inc., Wallingford.

[28] Becke, D. (1986) Density Functional Calculations of Molecular Bond Energies. *The Journal of Chemical Physics*, **84**, 4524-4529. https://doi.org/10.1063/1.450025

[29] Lee, C., Yang, W. and Parr, R.G. (1988) Development of the Colle-Salvetti Correlation-Energy Formula into a Functional of the Electron Density. *Physical Review B*, **37**, 785-789. https://doi.org/10.1103/PhysRevB.37.785

[30] Koopmans, T. (1934) Über die Zuordnung von Wellenfunktionen und Eigenwerten zu den Einzelnen Elektronen Eines Atoms. *Physica*, **1**, 104-113. https://doi.org/10.1016/S0031-8914(34)90011-2

[31] Saha, S.K., Ghosh, P., Hens, A., Murmu, N.C. and Banerjee, P. (2015) Density Functional Theory and Molecular Dynamics Simulation Study on Corrosion Inhibition Performance of Mild Steel by Mercapto-Quinoline Schiff Base Corrosion Inhibitor. *Physica E*: *Low-Dimensional Systems and Nanostructures*, **66**, 332-341. https://doi.org/10.1016/j.physe.2014.10.035

[32] Robert, G., Parr László, Szentpály, V. and Shubin, L. (1999) Electrophilicity Index. *Journal of the American Chemical Society*, **121**, 1922-1924. https://doi.org/10.1021/ja983494x

[33] Becke, A.D. (1996) Density-Functional Thermochemistry. IV. A New Dynamical Correlation Functional and Implications for Exact-Exchange Mixing. *The Journal of Chemical Physics*, **104**, 1040-1046. https://doi.org/10.1063/1.470829

[34] Michaelson, H.B. (1977) The Work Function of the Elements and Its Periodicity. *Journal of Applied Physics*, **48**, 4729-4733. https://doi.org/10.1063/1.323539

[35] Dewar, M.J.S., Zoebisch, E.G., Healy, E.F. and Stewart, J.P. (1985) Development and Use of Quantum Mechanical Molecular Models, 76, AM1: A New General Purpose Quantum Mechanical Molecular Model. *Journal of the American Chemical Society*, **107**, 3902-3909. https://doi.org/10.1021/ja00299a024

[36] Berrissoul, A., Ouarhach, A., Benhiba, F., *et al.* (2020) Evaluation of *Lavandula mairei* Extract as Green Inhibitor for Mild Steel Corrosion in 1 M HCl Solution. Experimental and Theoretical Approach. *Journal of Molecular Liquids*, **313**, Article ID: 113493. https://doi.org/10.1016/j.molliq.2020.113493

[37] Morell, C., Grand, A. and Toro-Labbé, A. (2005) New Dual Descriptor for Chemical Reactivity. *Journal of Physical Chemistry A*, **109**, 205-212. https://doi.org/10.1021/jp046577a

[38] Martínez-Araya, J.I. (2015) Why Is the Dual Descriptor a More Accurate Local Reactivity Descriptor than Fukui Functions. *Journal of Mathematical Chemistry*, **5**, 451-465. https://doi.org/10.1007/s10910-014-0437-7

[39] Ahmed, R.K. and Zhang, S. (2020) Bee Pollen Extract as an Eco-Friendly Corrosion Inhibitor for Pure Copper in Hydrochloric Acid. *Journal of Molecular Liquids*, **316**, Article ID: 113849. https://doi.org/10.1016/j.molliq.2020.113849

[40] Fouda, A.S., Ismail, M.A., Khaled, M.A., *et al.* (2022) Experimental and Computational Chemical Studies on the Corrosion Inhibition of New Pyrimidinone Derivatives for Copper in Nitric Acid. *Scientific Reports*, **12**, Article ID: 16089. https://doi.org/10.1038/s41598-022-20306-4

[41] Qiang, Y., *et al.* (2017) Three Indazole Derivatives as Corrosion Inhibitors of Copper in a Neutral Chloride Solution. *Corrosion Science*, **126**, 295-304. https://doi.org/10.1016/j.corsci.2017.07.012

[42] Benzbiria, N., Echihi, S., M.E.Belghiti, M.E., Thoume, A., Elmakssoudi, A., Zarrouk, A., Zertoubi, M. and Azzi, M. (2021) Novel Synthetized Benzodiazepine as Efficient Corrosion Inhibitor for Copper in 3.5% NaCl Solution. *Materials Today*: *Proceedings*, **37**, 3932-3939. https://doi.org/10.1016/j.matpr.2020.09.030

[43] Abdallah, M., Alfakeer, M., Amal Alonazi, M.S. and Al-Juaid, S. (2019) Ketamine Drug as an Inhibitor for the Corrosion of 316 Stainless Steel in 2M HCl Solution. *International Journal of Electrochemical Science.* **14**, 10227-10247. https://doi.org/10.20964/2019.11.10

[44] Beda, R.H.B., Tigori, M.A., Diabaté, D. and Niamien, P.M. (2021) Anticorrosive Properties of Theophylline on Aluminium Corrosion in 1 M HCl: Experimental, and Computational Assessment of Iodide Ions Synergistic Effect. *Current Physical Chemistry*, **11**, 227-242. https://doi.org/10.2174/1877946811666210526152314

[45] Brahim, A.A., Brahim, E.I., Abdelaziz, A.A., Abdul, S. and El-Habib, A.A. (2021) Assessment of Corrosion Inhibition Performance and Adsorption Thermodynamics of Hydrogen Phosphate (HPO_4^{2-}) and Molybdate (MoO_4^{2-}) Oxyanions on Tin in Maleic Acid. *Electroanalysis*, **33**, 804-819. https://doi.org/10.1002/elan.202060581

[46] Lazrak, J., Arrousse, N., El-Hajjaji, F., *et al.* (2021) Origanum Compactum Essential Oil as a Green Inhibitor for Mild Steel in 1 M Hydrochloric Acid Solution: Experimental and Monte Carlo Simulation. *Materials Today*: *Proceedings*, **45**, 7486-7493. https://doi.org/10.1016/j.matpr.2021.02.233

[47] Jmiai, A., Tara, A., Jbara, O., Bazzi, L., *et al.* (2021) A New Trend in Corrosion Protection of Copper in Acidic Medium by Using Jujube Shell Extract as an Effective Green and Environmentally Safe Corrosion Inhibitor: Experimental, Quantum Chemistry Approach and Monte Carlo Simulation Study. *Journal of Molecular Liquids*, **322**, Article ID: 114509. https://doi.org/10.1016/j.molliq.2020.114509

[48] Rouifi, Z., Rbaa, M., Abousalem, A.S., Benhiba, F., Laabaissi, T., Oudda, H., Lakhrissi, B. Guenbour, A., Warad, I. and Zarrouk, A. (2020) Synthesis, Characterization and Corrosion Inhibition Potential of Newly Benzimidazole Derivatives: Combining Theoretical and Experimental Study. *Surfaces and Interfaces*, **18**, Article ID: 100442. https://doi.org/10.1016/j.surfin.2020.100442

[49] Rahmani, H., Alaoui, K.I., EL Azzouzi, M., Benhiba, F., El Hallaoui, A., Rais, Z., Taleb, M., Saady, A., Labriti, B., Aouniti, A. and Zarrouk, A. (2019) Corrosion Assessment of Mild Steel in Acid Environment Using Novel Triazole Derivative as a Anti-Corrosion Agent: A Combined Experimental and Quantum Chemical Study. *Chemical Data Collections*, **24**, Article ID: 100302. https://doi.org/10.1016/j.cdc.2019.100302

[50] Adejo, S.O. and Ekwenchi, M.M. (2014) Resolution of Adsorption Characterisation Ambiguity through the Adejo-Ekwenchi Adsorption Isotherm: A Case Study of Leaf Extract of *Hyptis suaveolens* Poit as Green Corrosion Inhibitor of Corrosion of Mild Steel in 2 M HCl. *Journal of Emerging Trends in Engineering and Applied Sciences*, **5**, 201-205. https://hdl.handle.net/10520/EJC157010

[51] Heba, E.H., Ahmed, A.F., Eslam, A.M. and Eman, M.A. (2022) Experimental and Theoretical Assessment of Benzopyran Compounds as Inhibitors to Steel Corrosion in Aggressive Acid Solution. *Journal of Molecular Structure*, **1249**, Article ID: 131641. https://doi.org/10.1016/j.molstruc.2021.131641

[52] Abdallah El, A., Aaziz, J., Moutie, M.R., Rachid, O., Khalid, A., Hanane, Z., Musta-

pha, H., Hassan, B., Lahcen, B. and Souad El, I. (2022) Computational and Experimental Studies of the Inhibitory Effect of Imidazole Derivatives for the Corrosion of Copper in an Acid Medium. *Journal of Molecular Liquids*, **345**, Article ID: 117813. https://doi.org/10.1016/j.molliq.2021.117813

[53] Gadow, H.S., Thoraya, A.F. and Eldesoky, A.M. (2019) Experimental and Theoretical Investigations for Some Spiropyrazoles Derivatives as Corrosion Inhibitors for Copper in 2 M HNO_3 Solutions. *Journal of Molecular Liquids*, **294**, Article ID: 111614. https://doi.org/10.1016/j.molliq.2019.111614

[54] Henry, U.N., Ekemini, D.A., Lukman, Olasunkanmi, O., Chandrabhan, V., Amal Al-Mohaimeed, M., Dunia, A.A. and Ebenso, E.E. (2021) N-Substituted Carbazoles as Corrosion Inhibitors in Microbiologically Influenced and Acidic Corrosion of Mild Steel: Gravimetric, Electrochemical, Surface and Computational Studies. *Journal of Molecular Structure*, **122**, Article ID: 129328. https://doi.org/10.1016/j.molstruc.2020.129328

[55] Dheeraj, S.C., Chandrabhan, V. and Quraishi, M.A. (2021) Molecular Structural Aspects of Organic Corrosion Inhibitors: Experimental and Computational Insights. *Journal of Molecular Structure*, **1227**, Article ID: 129374. https://doi.org/10.1016/j.molstruc.2020.129374

[56] Razieh, F., Behzadi, H., Morteza Mousavi-Khoshdel, S.M. and Ali Ghaffarinejad, A. (2020) Evaluation of Corrosion Inhibition of 4-(pyridin-3-yl)thiazol-2-amine for Copper in HCl by Experimental and Theoretical Studies. *Journal of Molecular Structure*, **1205**, Article ID: 127658. https://doi.org/10.1016/j.molstruc.2019.127658

[57] Yin, D., *et al.* (2021) Theoretical and Electrochemical Analysis on Inhibition Effects of Benzotriazole Derivatives (un- and methyl) on Copper Surface. *Journal of Molecular Structure*, **1243**, Article ID: 130871. https://doi.org/10.1016/j.molstruc.2021.130871

[58] Shariatinia, Z. and Ahmadi-Ashtiani, A. (2019) Corrosion Inhibition Efficiency of Some Phosphoramide Derivatives: DFT Computations and MD Simulations. *Journal of Molecular Liquids*, **292**, Article ID: 111409. https://doi.org/10.1016/j.molliq.2019.111409

[59] Lukman, O.O. and Eno, E.E. (2020) Experimental and Computational Studies on Propanone Derivatives of Quinoxalin-6-yl-4,5-dihydropyrazole as Inhibitors of Mild Steel Corrosion in Hydrochloric Acid. *Journal of Colloid and Interface Science*, **561**, 104-116. https://doi.org/10.1016/j.jcis.2019.11.097

[60] Zhang, J., Li, W., Zuo, X., Chen, Y., Luo, W., Zhang, Y., Fu, A., Tan, B. and Zhang, S. (2021) Combining Experiment and Theory Researches to Insight into Anticorrosion Nature of a Novel Thiazole Derivative. *Journal of the Taiwan Institute of Chemical Engineers*, **122**, 190-200. https://doi.org/10.1016/j.jtice.2021.04.035

[61] Tigori, M.A., Kouyaté, A., Kouakou, V., Niamien, P.M. and Trokourey, A. (2020) Computational Approach for Predicting the Adsorption Properties and Inhibition of Some Antiretroviral Drugs on Copper Corrosion in HNO_3. *European Journal of Chemistry*, **11**, 235-244. https://doi.org/10.5155/eurjchem.11.3.235-244.2011

[62] Vandana, S., Mahendra, Y. and Obot, I.B. (2020) Investigations on Eco-Friendly Corrosion Inhibitors for Mild Steel in Acid Environment: Electrochemical, DFT and Monte Carlo Simulation Approach. *Colloids and Surfaces A*: *Physicochemical and Engineering Aspects*, **599**, Article ID: 124881. https://doi.org/10.1016/j.colsurfa.2020.124881

[63] Vranda, K.S., Pushyaraga, P.V., Reena Kumari, P.D. and Debashree, C. (2021) Effective Inhibition of Mild Steel Corrosion by 6-bromo-(2,4-dimethoxyphenyl) methylidene]imidazo[1,2-a]pyridine-2-carbohydrazide in 0.5 M HCl: Insights from

Experimental and Computational Study. *Journal of Molecular Structure*, **1232**, Article ID: 130074. https://doi.org/10.1016/j.molstruc.2021.130074

[64] Khattabi, M., Benhiba, F., Tabti, S., Djedouani, A., El Assyry, A., Touzani, R., Warad, I., Oudda, H. and Zarrouk, A. (2019) Performance and Computational Studies of Two Soluble Pyran Derivatives as Corrosion Inhibitors for Mild Steel in HCl. *Journal of Molecular Structure*, **1196**, 231-244. https://doi.org/10.1016/j.molstruc.2019.06.070

[65] Nuha, A.W., Obot, I.B. and Kaya, S.S. (2016) Theoretical Modeling and Molecular Level Insights into the Corrosion Inhibition Activity of 2-Amino-1,3,4-thiadiazole and Its 5-Alkyl Derivatives. *Journal of Molecular Liquids*, **221**, 579-602. https://doi.org/10.1016/j.molliq.2016.06.011

[66] Berrissoul, A., Ouarhach, A., Benhiba, F., Romane, A., Zarrouk, A., Guenbour, A., Dikici, B. and Dafali, A. (2020) Evaluation of *Lavandula mairei* Extract as Green Inhibitor for Mild Steel Corrosion in 1 M HCl Solution. Experimental and Theoretical Approach. *Journal of Molecular Liquids*, **313**, Article ID: 113493. https://doi.org/10.1016/j.molliq.2020.113493